# Mitigating Peak-to-Average Power Variability in Wave Energy Converter Systems: A Design Comparison


Derek Jackson
School of Electrical Engineering and Computer Science
Oregon State University
Corvallis, Oregon, USA
jacksder@oregonstate.edu

Chris Dizon
School of Electrical Engineering and Computer Science
Oregon State University
Corvallis, Oregon, USA
dizonc@oregonstate.edu

Mohamad Saad Mohamad Khalid Shaikh
School of Electrical Engineering and Computer Science
Oregon State University
Corvallis, Oregon, USA
shaikhm@oregonstate.edu

Yue Cao
School of Electrical Engineering and Computer Science
Oregon State University
Corvallis, Oregon, USA
yue.cao@oregonstate.edu

Ted Brekken
School of Electrical Engineering and Computer Science
Oregon State University
Corvallis, Oregon, USA
brekken@engr.orst.edu

Anna Edwards
Electrical Engineering
Oscilla Power, Inc.
Seattle, Washington, USA
edwards@oscillapower.com



***Abstract*—Ocean wave energy converters (WEC) with rotary drivetrains may use onboard energy storage to reduce the undesirable, large peak-to-average power ratio (PAPR) for grid-connected operation. The current energy storage system used in the Triton-C WEC developed by Oscilla Power, Inc. utilizes a bank of supercapacitors (SC) connected directly to the DC bus between the onboard AC/DC and DC/AC inverters. Contrary to this configuration, the majority of literature uses a DC/DC converter to connect the SC to the DC bus. This paper compares the two designs to determine which configuration is optimal in terms of PAPR mitigation and cost. Comparison is performed through simulations using field-based data and models. The work finds that while a DC/DC converter allows a higher utilization of the SC energy capacity, the cost of a multi-MW rated DC/DC converter outweighs the cost savings of the reduced energy storage size.**



***Keywords*—Wave Energy Converter, Wave to Grid, Peak Power Shaving, Supercapacitor, Energy Storage Sizing, Energy Management.**


## I. Introduction

A well-known challenge with ocean wave energy devices is that there is intrinsically large peak-to-average power variability. Ocean wave energy converters (WEC) may employ a hydraulic power dissipation network and onboard energy storage to substantially mitigate the peak-to-average power ratio (PAPR) to improve the output power quality and reduce the short-term variability. Supercapacitors (SC) are a popular choice for energy storage on WECs due to their fast transients, long lifetime, and high power density [1]. The current SC design used in the Triton-C WEC developed by Oscilla Power, Inc. (OPI), deployed in summer 2022 at the WETS test site in Hawaii, uses a direct-coupled SC system. The goal of this research is to determine if a DC/DC converter regulated SC offers benefits over the direct-coupled SC system.

Ocean waves are irregular and slow (e.g., periods of ~10 s) and produce varying power output from the WEC that results in poor coupling with the grid [2]. A standard WEC has a PAPR ratio of 10:1 to 15:1, depending upon the sea tides and weather [3]. A substantial reduction of the PAPR is crucial for WECs to provide the most benefit to the grid. The period and short-term power variability of ocean waves are well-suited for SC-based energy storage, which has a similar high-power charge-discharge period of 1-100 seconds [4],[5].

Many SC-integrated renewable energy systems in the literature use a DC/DC converter to connect the SC bank [5]-[12]. However, converters in the literature are designed for much lower power ratings than a typical WEC of 100s kW

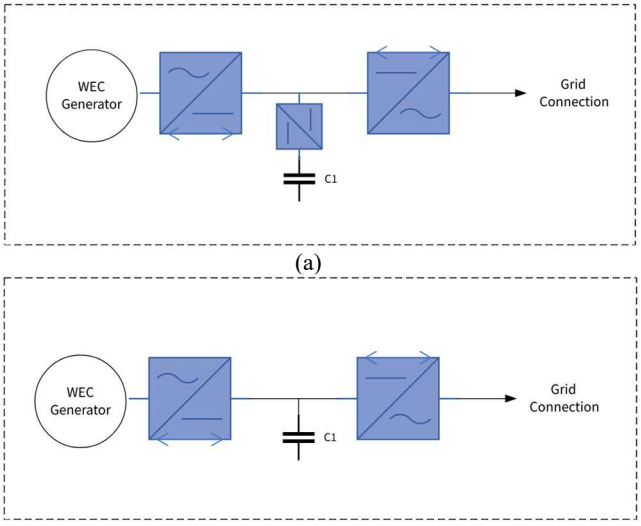


Fig. 1. Electrical system one line for fixed bus operation with DC/DC converter (a), and variable bus operation (b).


The authors gratefully acknowledge the US Department of Energy, the Pacific Ocean Energy Trust (POET), and the TEAMER program for supporting and funding this work.



978-1-6654-6618-9/22/$31.00 ©2022 IEEE

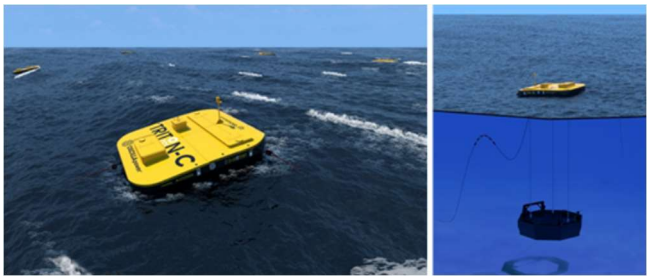

Fig. 2. OPI's Triton-C wave energy converter.

to MW levels, requiring larger and more expensive converters. Since a DC/DC converter must be sized for the peak power, the high PAPR of wave energy may cause the traditional DC/DC converter approach to be suboptimal. Little literature exists on WEC PAPR mitigation using a SC directly connected to the DC bus, where one paper focused on lab-based experiments to characterize the SC modules [13]. Additionally, no literature was found comparing these two designs. By performing a direct comparison between these two designs, this research could change or verify the way these systems are currently designed.

This paper focuses on validating and sizing two designs of an onboard SC energy storage system to help choose the optimal solution for a WEC. A numerical analysis using field-based data will compare the two designs. Design 1 (Fig. 1a) represents a fixed voltage DC bus operation in which the SC energy storage is connected to the common DC bus through a DC/DC converter. Design 2 (Fig. 1b) represents a variable voltage bus operation, in which the SC is connected directly to the common DC bus and is currently implemented on the Triton-C. The PAPR, cost, and energy delivered to the grid for the two systems will be compared to determine the preferred onboard SC power-smoothing system for a WEC.

## II. WEC System Modeling

OPI's field data is used to construct the WEC power generation model discussed in Section II-A and the electrical models in Section III. Because the WEC under consideration is rated at a few mega-watts, hardware validation is impractical due to costs, among other challenges.

### A. WEC Power Generation

The Triton-C (Fig. 2) consists of a surface float and a vertically asymmetric heave-plate connected by three tendons. It operates in multiple modes of motion (primarily heave and pitch, but also roll, surge and sway), allowing it to capture energy from waves across a wide range of ocean conditions. Drivetrains in the surface float convert the captured mechanical energy into electrical energy with very high efficiency and reliability. OPI has generated their WEC data in OrcaFlex for the dynamics and power, resulting in two different irregular sea states A and B. Sea state A data was generated for a peak period of 7.7 s and a significant wave height of 2.75 m. Sea state B data was generated for a peak period of 14.8 s and a significant wave height of 4.25 m. Both sea states utilize a Bretschneider spectrum to generate the wave profile. The time series power data shown in Fig. 3 is provided as the input to the WEC energy storage system, allowing the hydrodynamics to remain as a black box. The PAPR for sea states A and B of Fig. 3 are approximately 10 and 15, respectively.

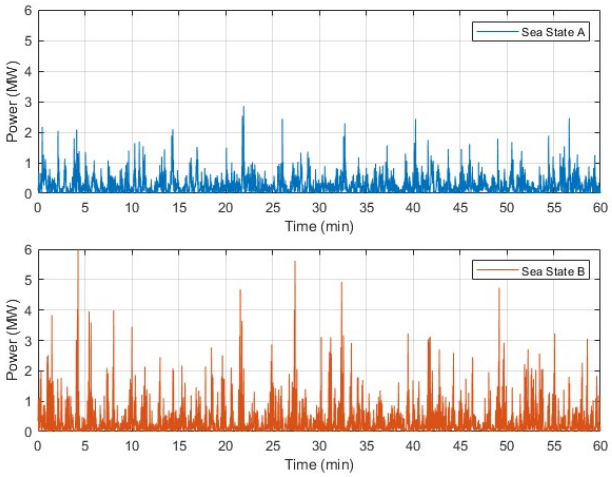


Fig. 3. WEC power time series for sea states A and B.

### B. Design 1: Regulated DC Bus

In Design 1, a DC/DC converter regulates the power flow between the DC bus and the SC energy storage (see Fig. 1a). This allows more utilization of the energy stored in the SC in addition to the DC bus voltage to be a design variable, rather than floating with the energy storage. Further discussion on energy storage utilization can be found in Section IV. The generator-side AC/DC converter, energy storage DC/DC converter, and grid-side DC/AC converter are all connected to the common DC bus.

### C. Design 2: Variable DC Bus

Design 2 has the SC energy storage directly connected to the DC bus (see Fig. 1b). While this is a less complex system topology, it also causes the DC bus voltage to vary with the amount of stored energy in the SC. Both the DC/AC and AC/DC converters must then be capable of operating across the entire SC voltage range.

### D. Peak Power Reduction Controls

While the system topologies for Designs 1 and 2 are different, their power flows are effectively the same. This allows the same power controller to be used for both design configurations. The control diagram is shown in Fig. 4. For each design, the power delivered to the grid $P_{grid}$ is the summation of the generated power $P_{gen}$ and power from the energy storage $P_{es}$ (i.e., $P_{grid} = P_{gen} + P_{es}$). Reducing the

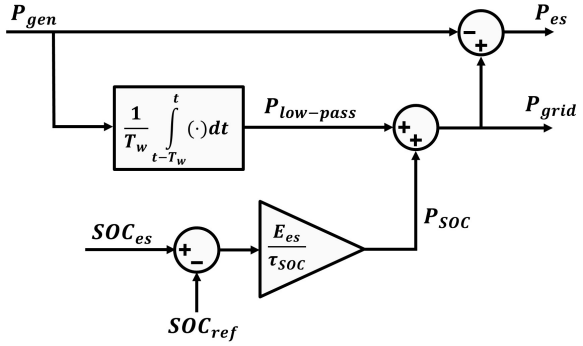


Fig. 4. Power control diagram to distribute WEC generated power between the energy storage and the grid.

peak value of $P_{grid}$ is achieved by averaging $P_{gen}$ over a time period of $T_w$. This time-window averaging unit acts as a low-pass filter using the energy storage to smooth out the generated power waveform. By increasing $T_w$, $P_{gen}$ is averaged over a longer period which can further smooth out the PAPR of $P_{grid}$. However, the required energy storage capacity increases with $T_w$, incurring larger design costs. The power controller also includes a SOC correction factor, which pushes the energy storage SOC to a reference value $SOC_{ref}$ under steady-state conditions. The correction factor time constant $\tau_{SOC}$ controls the rate at which the energy storage SOC reaches $SOC_{ref}$, and is scaled by the max energy capacity of the SC $E_{es}$ to achieve a correction factor in watts.

The proposed power controller could likely be implemented in hardware several different ways. However, one implementation approach will be discussed. For both Design 1 and Design 2, the $P_{grid}$ output of the power controller would serve as an input to a direct power control scheme for the grid-connected DC/AC inverter. In the case of the variable DC bus of Design 2, no additional hardware controls are necessary. The DC/DC controls for Design 1 could simply regulate the DC bus voltage to a constant value. As the input power $P_{gen}$ and output power $P_{grid}$ will affect the DC bus voltage (assuming a DC-link capacitance exists), $P_{es}$ will be implicitly implemented. WEC-side controls are omitted because the WEC-connected AC/DC converter is accounted for in the power generation waveforms discussed in Section II-A.

## III. Component Models and Sizing

In the context of this design comparison, the system performance and cost using currently available and manufactured equipment is of interest. Since manufacturers rarely reveal converter design details (e.g., semiconductors devices, switching frequency, thermal management, etc.), the use of high-fidelity models that require such information would provide little benefit. Therefore, experimentally-derived or datasheet-based models are used for the SC and inverter. Given the absence of DC/DC converter performance data at the required power ratings of the WEC system, the DC/DC converter is modeled with a constant efficiency of 97%. Section IV includes discussion on how results are impacted by the DC/DC converter model.

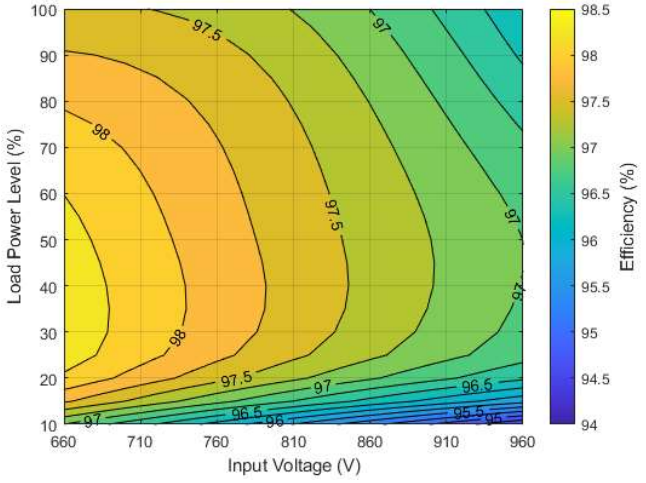


Fig. 5. DC/AC inverter efficiency map dependent on input voltage and normalized power level.

### A. Supercapacitor Model

The SC energy storage is represented by the classic SC model provided in [14] which consists of a single storage element, conduction loss resistance, and self-discharge resistance. The dynamic behavior is dependent on four parameters: rated voltage $V_{rated}$, total capacitance $C$, equivalent series resistance $R_s$, and parallel (self-discharge) resistance $R_p$. These four parameters are commonly provided in the manufacturer's datasheet, where a SkelMod SMA102V88FAF supercapacitor is used in this paper's study. Scaling of the SC energy capacity is achieved by connecting multiple SC modules in series $N_s$ and parallel $N_p$, where the total energy capacity is given by

$$E_{es} = N_s \cdot N_p \cdot \frac{1}{2} C V_{rated}^2 \tag{1}$$

### B. DC/AC Inverter Model

To model the inverter, an efficiency vs. load and voltage curve is used to calculate realistic losses, implemented as a lookup table for the simulations. The performance data was obtained from the dataset experimentally collected by the California Energy Commission which includes over 3,000 inverters [15]. Performance characteristics were depicted as a function of power level and DC input voltage, providing measurements at three voltage levels and six power levels. Inverters on the list were down-selected to those that met input voltage ranges of 660-960 V (based on system specification) and maximum continuous output power ranges of 300-500 kW. The resulting efficiency map is shown in Fig. 5.

## IV. WEC Simulations

The WEC energy storage optimization presented in this paper considers two design variables: energy storage size $E_{es}$, and the controller time-window period $T_w$. Optimal sizing and controller settings are found through an exhaustive search of the design space, sweeping through a range of $E_{es}$ and $T_w$. The energy storage capacity $E_{es}$ is adjusted by increasing the number of SC modules in parallel $N_p$ while the number of SC modules in series $N_s$ is held constant. Each candidate design is evaluated for total system cost $C$ given a maximum PAPR and various electrical

TABLE I. Design Constraints.

| *Design* | *Constraint* | *Limits* |
|---|---|---|
| 1 | SC bank voltage (V) | $204 \leq V_{es} \leq 1020$ |
| | SC bank SOC | $0 \leq SOC_{es} \leq 1$ |
| | SC bank charge/discharge current (A) | $I_{es} \leq 2689 \cdot N_p$ |
| 2 | SC bank voltage (V) | $660 \leq V_{es} \leq 960$ |
| | SC bank SOC | $0 \leq SOC_{es} \leq 1$ |
| | SC bank charge/discharge current (A) | $I_{es} \leq 2689 \cdot N_p$ |

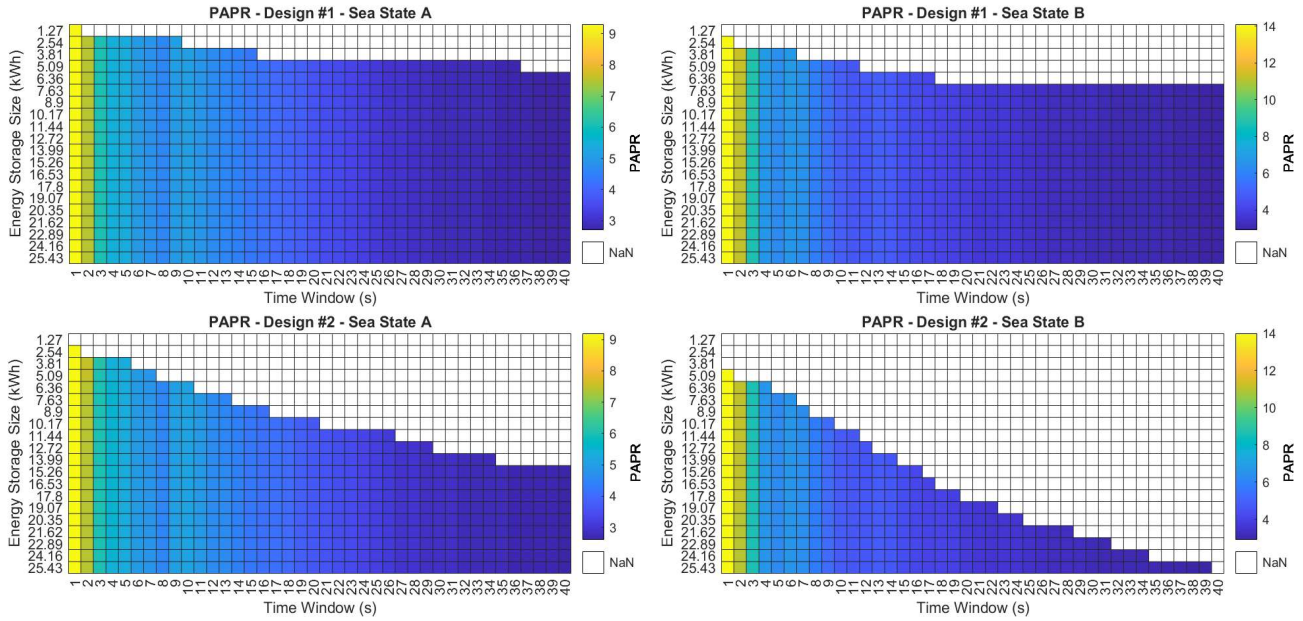


Fig. 6. Maximum PAPR vs. $E_{es}$ and $T_w$ for both design configurations and sea states.

operation constraints, given in Table I. The cost functions are given in the following subsection.

The voltage limits in Table I are the same for every parameter combination as the SC bank voltages are held constant for all designs. Design 1 upper voltage limit is based on the rated voltage of the SkelMod SC, scaled by $N_s = 10$, whereas the lower limit was defined as 20% of the max voltage limit. Design 2 voltage limits are based on the operating range of the DC/AC inverter. The current limits in Table I use the rated current found on the SkelMod SC datasheet scaled by $N_p$. Using data provided by the industry, this approach can inform engineers on future design improvements of the WEC energy storage system.

### A. Component Pricing

To evaluate the costs of all electrical components, price models were created using databases for variable frequency drives (VFDs) and SCs. VFDs were used based on the assumption that costs were of similar value to those of WEC-compatible inverters and converters. VFD data was collected for power ratings within 37-372 kW (50-500 HP) among Eaton, Fuji, and Schneider Electric manufacturers [16]. The model is best represented by the linear equation (2), relating price in \$ ($y$) and rated power in kW ($x$).

$$y = 134x + 1349.3 \tag{2}$$

For the SC price model, data was collected with rated voltages equal to or above the already considered 102 V SkelMod SC [17]. Manufacturers included SkelMod, LICAP, and Eaton. The model is best represented by the linear equation (3), relating price in \$ ($y$) and SC energy capacity in Wh ($x$).

$$y = 30.77x + 324 \tag{3}$$

### B. Design Cost and Performance Comparison

Design evaluation is performed in MATLAB/Simulink where Designs 1 and 2 are simulated for both sea states shown in Fig. 3. A total of 800 design variable combinations were simulated for both Design 1 and Design 2 and for both sea states. Energy storage capacity $E_{es}$ ranged from 1 kWh to 20 kWh, and $T_w$ ranged from 1 s to 40 s. Fig. 6 shows the resulting PAPR for all combinations of $E_{es}$, $T_w$, sea state, and design configuration. A white cell denotes an infeasible design with too little ES capacity. The control variable $T_w$ has the greatest impact on PAPR, since it affects the power averaging of the energy storage. The capacity $E_{es}$ then correlates to how large a $T_w$ can be used. This is attributed to

TABLE II. TOP CONFIGURATIONS FOR DESIGNS 1 AND 2 FOR $PAPR < 3$ AND $PAPR < 5$.

| *Sea State* | *Design* | *PAPR* | *Total Cost ($)* | *SC Cost ($)* | *DC/AC Cost ($)* | *DC/DC Cost ($)* | $T_w$ *(s)* | $E_{es}$ *(kWh)* | $E_{grid}$ *(kWh)* |
|---|---|---|---|---|---|---|---|---|---|
| A | 1 | 2.86 | 561k | 157k | 106k | 298k | 34 | 5.09 | 273 |
| | | 4.62 | 508k | 79k | 170k | 259k | 8 | 2.54 | 272 |
| | 2 | 2.92 | 502k | 392k | 110k | - | 29 | 12.72 | 279 |
| | | 4.78 | 336k | 157k | 179k | - | 7 | 5.09 | 277 |
| B | 1 | 2.91 | 1084k | 235k | 144k | 705k | 39 | 7.63 | 367 |
| | | 4.75 | 991k | 157k | 234k | 600k | 11 | 5.09 | 366 |
| | 2 | 2.87 | 930k | 783k | 147k | - | 39 | 25.43 | 379 |
| | | 4.66 | 589k | 352k | 237k | - | 11 | 11.44 | 377 |

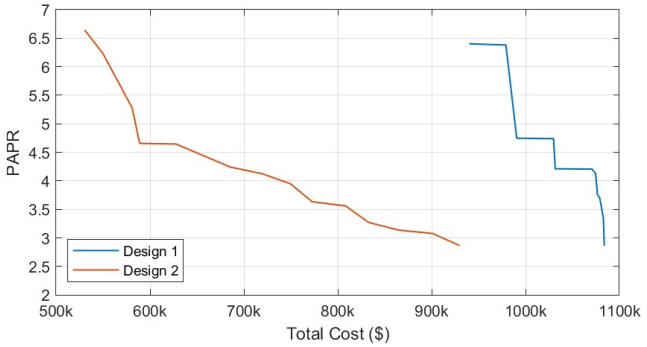

Fig. 7. PAPR vs. total system cost of Designs 1 and 2 for sea state B.

the averaging approach used in the peak power reduction controller.

The major benefit of Design 1 is the decoupling of the inverter input voltage range and the SC voltage. This allows greater utilization of the energy storage, where 96% of the available energy storage is used. Whereas Design 2 utilizes only 52.7%. The greater energy storage utilization of Design 1 over Design 2 can also be observed in Fig. 6. For the same $T_w$, Design 1 requires approximately half of the energy storage size as Design 2 for both sea states.

Table II summarizes the results of the lowest cost configurations for each design and sea state, while achieving a $PAPR < 3$ and $PAPR < 5$. Note that the PAPR values are not exactly the same for each design configuration. Since the PAPR does not monotonically decrease with an increasing $T_w$, it is possible for a design with a lower PAPR to be cheaper than a design with a higher PAPR. The PAPR limits selected for Table II are just samples to provide a more in-depth quantitative comparison between the two design comparisons. Ultimately the PAPR limit would be discussed with the local utility company to determine the optimal PAPR for grid services.

While Design 2 utilizes around 50% of the available energy stored in the SC, it actually is the cheaper design option. This is observed in Table II. Since Design 2 does not include a DC/DC converter, the overall system cost is less than Design 1. Even though Design 2 requires 2-4 times the energy storage capacity of Design 1, the lower cost of energy storage is not enough to compensate for the cost of the DC/DC converter. The cost difference for the same PAPR can also be inferred from Fig. 7, which shows the PAPR vs. total system cost for Designs 1 and 2. Interestingly, the PAPR rate of change over cost is overall more gradual for Design 2 than Design 1. This suggests there exists a PAPR where Design 1 becomes the more cost-effective option – provided the intersection occurs before unity PAPR.

The total energy delivered to the grid $E_{grid}$ is another important detail to consider, and is included in Table II. Simulating Design 2 results in an $E_{grid}$ 3% larger than Design 1. Note that this exact difference is not entirely accurate due to the fixed-efficiency DC/DC converter model used. However, it can be concluded that no DC/DC converter will result in a higher $E_{grid}$. While Design 1 enables the inverter to operate with its maximum efficiency input voltage, the *total* system efficiency must be greater than Design 2 for a higher $E_{grid}$. To achieve a higher total efficiency than Design 2, the DC/DC converter would require an efficiency >99% at all operating points, which is likely infeasible or impractical in practice.

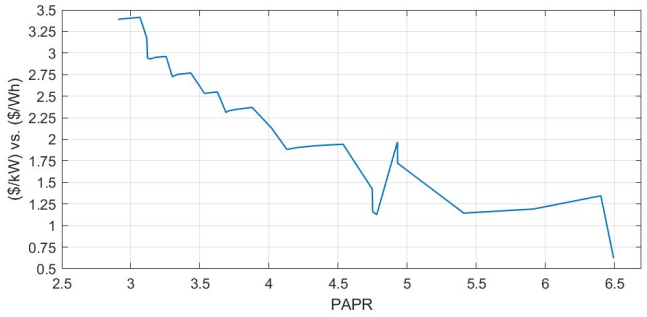

Fig. 8. The ratio between the $/kW of the DC/DC converter and $/Wh of the SC energy storage where the costs of Designs 1 and 2 are equivalent. The plot shows the ratio for a range of PAPR for sea state B. The price models presented in this paper results in a cost ratio of 4.36.

### C. *Alternative Component Pricing Analysis*

The results in Table II and in Fig. 7 are largely dependent on the cost models used, which are based on prices provided by online distributors gathered at the time of writing. These prices are likely subject to change in the future when the manufacturing of power electronics and SC becomes more cost efficient. Additionally, working directly with a power converter manufacturer could result in lower costs. To accommodate for these uncertainties, an alternative component pricing analysis is performed. The goal is to determine at what point does Design 1 have an equivalent cost to Design 2 for different DC/DC converter and SC price models. The change in pricing models is represented by a ratio between DC/DC converter $/kW and SC energy storage $/Wh. The AC/DC converter costs are similar between both designs and are thus omitted from this analysis.

For a range of PAPR, the $/kW vs. $/Wh ratio where Design 1 has an equivalent cost to Design 2 is shown in Fig. 8. This considers only sea state B as it has a higher initial PAPR. For reference, the $/kW vs. $/Wh ratio of the price models (1)-(2) presented in this paper is 4.36. Hence, for all PAPR, Design 1 is more costly. However, if the $/kW vs. $/Wh ratio drops below 2.5, for example, then Design 1 with DC-DC converter will be cheaper if PAPR is required to be less than 3.5. Again, the non-monotonicity of the PAPR for an increasing $T_w$ causes the plot of Fig. 8 to also be non-monotonic. There is a general trend that a lower PAPR requires a smaller reduction in DC/DC converter cost (with respect to the SC cost) for Design 1 to become the cheaper option. This was also inferred from Fig. 7, where the cost difference between the two designs is reduced as the PAPR decreases. However, Fig. 8 provides a more concise analysis quantifying the necessary component prices for the preferred design to become Design 1.

## V. Concluding Remarks and Future Work

This paper presented a design comparison between two WEC energy storage configurations that focused on the PAPR and total system cost. Design 1 uses a DC/DC converter to regulate the energy stored in the SC and the DC bus voltage. Design 2 has the SC connected directly to the DC bus, and is the current design of OPI's Triton-C WEC. Both designs were evaluated through simulations using

industry-based data. While the use of a DC/DC converter can result in higher utilization of the SC energy capacity, the cost of a DC/DC converter outweighs the savings in SC size. Additionally, the analysis concludes that Design 2 has a greater total system efficiency.

Given the multidisciplinary nature of a WEC, assumptions were made to simplify the system design study. Future work will investigate the impact of SC energy storage weight on power generation. Rather than a predefined generator power time series, inclusion of a WEC dynamics model can provide insight on how system weight and DC bus voltage affects the power generation. The cost model can also be improved as more manufacturers release information on DC/DC converter costs. PAPR can additionally be improved by adding storage co-located with a Wave Energy farm of devices.

## REFERENCES


[1] J. H. Prudell, A. Schacher, and K. Rhinefrank, "Direct drive ocean wave energy electric plant design methodology," in *Oceans*, 2012, pp. 1-7.

[2] B. Czech and P. Bauer, "Wave Energy Converter Concepts: Design Challenges and Classification," in *IEEE Industrial Electronics Magazine*, vol. 6, no. 4, pp. 4-16, 2012.

[3] Y.H Yu, E. Muljadi, and H. B. Karayaka, "Investigations into Balancing Peak-to-Average Power Ratio and Mean Power Extraction for a Two-Body Point-Absorber Wave Energy Converter," in *Advanced Analysis and Techniques of Wave Energy Conversion and Integrated Storage*, vol. 14, no. 12, 2021.

[4] A. Rufer, *Energy Storage: Systems and Components*, Boca Raton, FL, CRC Press, 2017, pp. 108-109.

[5] I. H. Panhwar, K. Ahmed, M. Seyedmahmoudian, A. Stojcevski, B. Horan, S. Mekhilef, A. Aslam, and M. Asghar, "Mitigating Power Fluctuations for Energy Storage in Wind Energy Conversion System Using Supercapacitors," in *IEEE Access*, vol. 8, no. 1, pp.189747-189760, 2020.

[6] S. Hazra and S. Bhattacharya, "Minimizing Reactive Current of a High Gain Dual Active Bridge Converter for Supercapacitor Based Energy Storage System Integration," in *Proc. IEEE Energy Conversion Congress and Exposition (ECCE)*, 2018, pp. 1-8.

[7] P. Moreno-Torres, M. Blanco, G. Navarro, and M. Lafoz, "Power smoothing system for wave energy converters by means of a supercapacitor-based energy storage system," in *Proc. European Conference on Power Electronics and Applications*, 2015, pp. 1-7.

[8] P. Bauer, J. A. Ferreira, R. Kessel, and K. T. Todorčević, "Bidirectional modular multilevel DC-DC converter control and loss modeling for energy extraction from Electro Active Polymer Wave Energy generator," in *Proc. IEEE ECCE Asia Downunder*, 2013, pp. 1-7.

[9] F. Xue, R. Yu, W. Yu, A. Q. Huang, and Y. Du, "A novel bi-directional DC-DC converter for distributed energy storage device," in *Proc. IEEE Applied Power Electronics Conference and Exposition (APEC)*, 2015, pp. 1-5.

[10] J.S. Artal-Sevil, J.A. Domínguez-Navarro, D. Martínez, and C. Bernal-Ruíz, "Control and Design of an IPOS DC-DC Converter applied to High Voltage DC Transmission in a Wave Energy Converter," in *Proc. Fourteenth International Conference on Ecological Vehicles and Renewable Energies (EVER)*, 2019, pp. 1-9.

[11] G. Rajapakse, S. Jayasinghe, A. Fleming, and M. Negnevitsky, "Grid Integration and Power Smoothing of an Oscillating Water Column Wave Energy Converter," in *Energies*, vol. 11, no. 7, pp. 1-19, 2018.

[12] D. Murray, M. Egan, J. Hayes, D. Sullivan, "Applications of Supercapacitor Energy Storage for a Wave Energy Converter System," in *Proc. European Wave and Tidal Energy Conference (EWTEC)*, 2009, pp. 1-10.

[13] D. B. Murray, J. G. Hayes, D. L. O'Sullivan and M. G. Egan, "Supercapacitor Testing for Power Smoothing in a Variable Speed Offshore Wave Energy Converter," in *IEEE Journal of Oceanic Engineering*, vol. 37, no. 2, pp. 301-308, 2012.

[14] L. Zhang, Z. Wang, X. Hu, F. Sun, and D. G. Dorrell, "A comparative study of equivalent circuit models of ultracapacitors for electric vehicles," in *Journal of Power Sources*, vol. 274, pp. 899-906, 2015.

[15] California Energy Commission, "Solar Equipment Lists", 2020. Accessed on: Jan. 5th, 2022. [Online]. Available: https://www.energy.ca.gov/programs-and-topics/programs/solar-equipment-lists

[16] Grainger, "Variable Frequency Drives", 2022. Accessed on: Jan. 7, 2022. [Online]. Available: https://www.grainger.com/category/motors/motor-drives-speed-controls/variable-frequency-drives-accessories/variable-frequency-drives

[17] Digi-Key Electronics, "Electric Double Layer Capacitors (EDLC), Supercapacitors", 2022. Accessed on: Jan. 7, 2022. [Online]. Available: https://www.digikey.com/en/products/filter/electric-double-layer-capacitors-edlc-supercapacitors/61